



# Antagonism of the Muscarinic Acetylcholine Type 1 Receptor Enhances Mitochondrial Membrane Potential and Expression of Respiratory Chain Components via AMPK in Human Neuroblastoma SH-SY5Y Cells and Primary Neurons

Farhana Naznin<sup>1,2</sup> · T. M. Zaved Waise<sup>1</sup> · Paul Fernyhough<sup>1,2</sup>

Received: 5 May 2022 / Accepted: 16 August 2022 / Published online: 25 August 2022  
© The Author(s) 2022

## Abstract

Impairments in mitochondrial physiology play a role in the progression of multiple neurodegenerative conditions, including peripheral neuropathy in diabetes. Blockade of muscarinic acetylcholine type 1 receptor ( $M_1R$ ) with specific/selective antagonists prevented mitochondrial dysfunction and reversed nerve degeneration in in vitro and in vivo models of peripheral neuropathy. Specifically, in type 1 and type 2 models of diabetes, inhibition of  $M_1R$  using pirenzepine or muscarinic toxin 7 (MT7) induced AMP-activated protein kinase (AMPK) activity in dorsal root ganglia (DRG) and prevented sensory abnormalities and distal nerve fiber loss. The human neuroblastoma SH-SY5Y cell line has been extensively used as an in vitro model system to study mechanisms of neurodegeneration in DRG neurons and other neuronal sub-types. Here, we tested the hypothesis that pirenzepine or MT7 enhance AMPK activity and via this pathway augment mitochondrial function in SH-SY5Y cells.  $M_1R$  expression was confirmed by utilizing a fluorescent dye, ATTO590-labeled MT7, that exhibits great specificity for this receptor.  $M_1R$  antagonist treatment in SH-SY5Y culture increased AMPK phosphorylation and mitochondrial protein expression (OXPHOS). Mitochondrial membrane potential (MMP) was augmented in pirenzepine and MT7 treated cultured SH-SY5Y cells and DRG neurons. Compound C or AMPK-specific siRNA suppressed pirenzepine or MT7-induced elevation of OXPHOS expression and MMP. Moreover, muscarinic antagonists induced hyperpolarization by activating the M-current and, thus, suppressed neuronal excitability. These results reveal that negative regulation of this  $M_1R$ -dependent pathway could represent a potential therapeutic target to elevate AMPK activity, enhance mitochondrial function, suppress neuropathic pain, and enhance nerve repair in peripheral neuropathy.

**Keywords** Axon · Diabetic neuropathy · Dorsal root ganglia · Mitochondria · OXPHOS · Plasma membrane potential

## Introduction

Muscarinic acetylcholine receptors (mAChRs) are members of the superfamily of G protein coupled receptors (GPCRs) and consist of five molecular subtypes ( $M_1$ – $M_5$ ) [1, 2].

These receptors are coupled to various signal transduction pathways where  $M_1$ ,  $M_3$ , and  $M_5$  couple with  $G_q$  to activate the inositol triphosphate ( $IP_3$ ) pathway, and the  $M_2$  and  $M_4$  receptors couple with  $G_i$  to inhibit adenylyl cyclase [3, 4]. The muscarinic acetylcholine type 1 receptor ( $M_1R$ ) regulates numerous fundamental functions of the central and peripheral nervous systems and has been targeted for the development of new therapeutic modalities and drugs [5–7]. A variety of molecules block  $M_1R$  activation including pirenzepine, which is a selective orthosteric receptor antagonist with high affinity [8], and muscarinic toxin 7 (MT7) which is a highly specific antagonist (or negative allosteric modulator) [9, 10].

Mitochondria are highly dynamic, energy generating organelles that are known to concentrate in regions of high energy demand [11, 12] and are densely packed in

✉ Paul Fernyhough  
pfernough@sbr.ca

Farhana Naznin  
FNaznin@sbr.ca

T. M. Zaved Waise  
TWaise@sbr.ca

<sup>1</sup> Division of Neurodegenerative Disorders, St Boniface Hospital Albrechtsen Research Centre, R4046 - 351 Taché Ave, Winnipeg, MB R2H 2A6, Canada

<sup>2</sup> Department of Pharmacology and Therapeutics, University of Manitoba, Winnipeg, MB, Canada

sensory nerve terminal boutons [13, 14]. Mitochondrial membrane potential (MMP) is a marker of optimal mitochondrial function where mitochondrial depolarization can indicate mitochondrial dysfunction [15–17]. Depolarization and the loss of MMP impacts respiratory chain complexes, which interrupts cellular electron flow and results in ATP depletion [18–21]. Maintenance of MMP is fundamental for the normal performance and survival of cells that have a high-energy requirement [22], such as sensory neurons [23–25]. Mitochondrial dysfunction and any energy deficit can contribute to the pathogenesis of neurodegenerative disease such as diabetic sensory neuropathy [23, 26, 27]. Furthermore, abnormal mitochondrial function correlated with a downregulation of mitochondrial proteins, including components of the respiratory chain complex [23, 26, 28]. Interestingly, blockade of M<sub>1</sub>R with pirenzepine or MT7 prevented mitochondrial dysfunction and reversed nerve degeneration in rodent models of diabetic neuropathy [29, 30].

The energy sensor AMP-activated protein kinase (AMPK)/peroxisome proliferator-activated receptor- $\gamma$  coactivator  $\alpha$  (PGC-1 $\alpha$ ) signaling pathway is linked to mitochondrial biogenesis and function [31, 32] and impaired AMPK/PGC-1 $\alpha$  signaling contributes to the aforementioned mitochondrial dysfunction and development of sensory neuropathy in diabetes [24, 30, 33–35]. Increased AMPK phosphorylation, driven by resveratrol or IGF-1, was associated with protection from neuropathy mediated via upregulation of respiratory chain components, augmentation of mitochondrial function, and respiratory complex activities [24, 36, 37]. We have recently shown in adult sensory neurons that pirenzepine and MT7 drive phosphorylation of AMPK mediated via Ca<sup>2+</sup> influx and activation of Ca<sup>2+</sup>/calmodulin-dependent protein kinase kinase  $\beta$  (CaMKK $\beta$ ) [29, 30]. This resulted in augmentation of mitochondrial function and elevated neurite outgrowth [29, 30, 38].

Neuronal hyperexcitability is a feature of neuropathic pain. The opening of potassium (K<sup>+</sup>) channels leads to hyperpolarization of the cell membrane which results in a decrease in cell excitability. K<sup>+</sup> channels, primarily Kv7.2/7.3 sub-types (termed M channels), regulate neuronal excitability in peripheral neurons and are modulated by a large array of receptor types [39–41]. The M-current (I<sub>M</sub>) is sensitive to the M<sub>1</sub>R agonist muscarine [42]. Muscarinic activation of M<sub>1</sub>R mobilizes internal Ca<sup>2+</sup> stores leading to closure of M channels and inducing a slow and long-lasting depolarization by inhibiting I<sub>M</sub> and this effect is usually accompanied by a decrease in membrane conductance [43, 44]. This muscarinic suppression of I<sub>M</sub> was antagonized by pirenzepine [45] through enhancing the I<sub>M</sub> current to make the neuron less excitable. However, the mechanistic interactions between antimuscarinic drug, mitochondrial membrane potential, and M-current remain to be defined.

Therefore, to advance understanding of the downstream consequences of M<sub>1</sub>R antagonism, we tested the hypothesis that M<sub>1</sub>R antagonism enhances mitochondrial function via activation of the AMPK signaling pathway as well as modulating neuronal excitability in human cells. This comprehensive study aimed at evaluating mitochondrial parameters including oxygen consumption rate (OCR), mitochondrial membrane potential (MMP), and expression of component proteins of the mitochondrial complexes (OXPHOS). We also investigated changes in plasma membrane potential in response to pirenzepine or MT7 in human neuroblastoma SH-SY5Y cells and primary neurons.

## Materials and Methods

### Animals and Cell Culture

The human neuroblastoma SH-SY5Y cell line (ATCC CRL-2266, Virginia, USA) was a kind gift from Dr. Jun-Feng Wang, University of Manitoba. The cells were cultured in DMEM/F12 (1:1) media supplemented with heat inactivated 10% FBS and 1X antibiotic antimycotic solution (A5955, Sigma, St. Louis, MO, USA).

Dorsal root ganglia (DRG) from adult male Sprague–Dawley rats were dissected and dissociated using previously described methods [29]. All animal procedures followed the guidelines of the University of Manitoba Animal Care Committee using the Canadian Committee on Animal Care (CCAC) rules. Neurons were cultured in defined Hams F12 media containing 10 mM D-glucose (N4888, Sigma) supplemented with modified Bottenstein's N2 additives (0.1 mg/ml transferrin, 20 nM progesterone, 100 mM putrescine, 30 nM sodium selenite, 0.1 mg/ml BSA; all additives were from Sigma). In all experiments, the media was also supplemented with 0.146 g/L L-glutamine, a low-dose cocktail of neurotrophic factors (0.1 ng/ml NGF, 1.0 ng/ml GDNF and 0.1 ng/ml NT-3; all from Promega, Madison, WI, USA), 0.1 nM insulin, and 1X antibiotic antimycotic solution. Cultures were treated with 100 nM MT7 (M-200, Alomone Labs, Jerusalem, Israel) or 1  $\mu$ M pirenzepine (P7412, Sigma).

### Localization of M<sub>1</sub>R

Fluorescent dye ATTO Fluor 590-conjugated MT7 (MT7-ATTO590; Alomone Labs) was used to detect M<sub>1</sub>R. The activity of this MT7-ATTO590 conjugate on M<sub>1</sub>R was confirmed by the company (Alomone Labs) in M<sub>1</sub>R/C6 cells by measuring intracellular changes in Ca<sup>2+</sup> levels and the specific binding was determined in rat DRG culture in the presence of excess (1  $\mu$ M) unlabeled MT7 (data not shown). Adult wild-type and M<sub>1</sub>R-KO (C57BL/6 background, line 1784; Taconic Biosciences Inc.) [46] mouse DRG tissues

were incubated with 100 nM MT7-ATTO590 containing media at 37 °C CO<sub>2</sub> incubator overnight and then fixed in 2% PFA, cryoprotected in 20% sucrose, and embedded in Tissue-Tek O.C.T. compound to prepare 7 µm sections. All sections were incubated overnight at 4 °C with β-tubulin III antiserum (1:500; T8578, Sigma) and then stained for 1 h with Alexa Fluor 488-conjugated anti-mouse IgG (1:1000; Invitrogen, California, USA) at room temperature. To confirm M<sub>1</sub>R expression in SH-SY5Y cells and cultured rat DRG neurons, cells/neurons were incubated with 100 nM MT7-ATTO590 at 37 °C in a CO<sub>2</sub> incubator overnight for microscopy. All images were taken by using a Carl Zeiss LSM510 confocal or AxioScope-2 fluorescence microscope.

### Small Interfering RNAs (siRNA)-Based Knockdown of AMPK

SH-SY5Y cells were transfected with 10 nM AMPK-specific siRNAs (AMPKα1, cat. 4392420, ID: s100 and s102; AMPKα2, cat. 4390824, ID: s11057, Thermo Scientific, Pittsburgh, PA, USA), or scrambled siRNA (cat. 4390843, Thermo Scientific) using Lipofectamine RNAiMAX (Invitrogen, Life Technologies, USA) according to the instruction manual. Briefly, siRNA was incubated with transfection reagent in Opti MEM (Invitrogen) for 5 min at room temperature to allow the formation of transfection complexes, and then the transfection complexes were added to cells drop-by-drop. Before transfection, the medium was changed to antibiotic-free DMEM. After 24 h of transfection, cells were changed to fresh medium and then subjected to various treatments as required.

### Quantitative Western Blotting

Cell lysate was harvested from cell culture and then homogenized in ice-cold RIPA buffer containing 25 mM Tris pH 8, 150 mM NaCl, 0.1% SDS, 0.5% sodium deoxycholate, 1% Triton X-100, and protease and phosphatase inhibitor cocktail. Protein assay was performed using the DC protein assay (Bio-Rad, CA, USA), and Western blot analysis was conducted. Proteins (15 µg total protein/lane) were resolved and separated via 10% sodium dodecyl sulfate–polyacrylamide gel electrophoresis (SDS-PAGE). The proteins were subsequently transferred to a nitrocellulose membrane (Bio-Rad) using Trans-Blot Turbo Transfer System (Bio-Rad) and immunoblotted with specific antibodies to phosphorylated AMPK (pAMPK on Thr172; 1:1000, Cell Signaling Technology, Massachusetts, USA), total AMPK (T-AMPK; 1:7000, Abcam, Cambridge, UK), total OxPhos (1:1000, Invitrogen; antibody cocktail containing multiple OxPhos antibodies against complex I (20 kDa), complex II (30 kDa), complex III (core 2; 48 kDa), complex IV (MTCO1 subunit, 40 kDa), and complex V (ATP5a subunit, 55 kDa)), NDUFS3 (1:1000, Abcam, complex I, 30 kDa), and total ERK

(T-ERK; 1:3000, Santa Cruz Biotechnology, Texas, USA). Of note, total protein bands were captured by chemiluminescent imaging of the blot after gel activation (TGX Stain-Free™ FastCast Acrylamide Solutions, Bio-Rad) in addition to the use of T-ERK levels for target protein normalization (to adjust for loading). The secondary antibodies were HRP-conjugated goat antirabbit IgG (H+L) or goat anti-mouse IgG (H+L) from Jackson ImmunoResearch Laboratories, PA, USA. The blots were incubated in Clarity™ Western ECL substrate (Bio-Rad) or SignalFire™ ECL Reagent (Cell Signaling Technology) and imaged using a Bio-Rad ChemiDoc image analyzer (Bio-Rad).

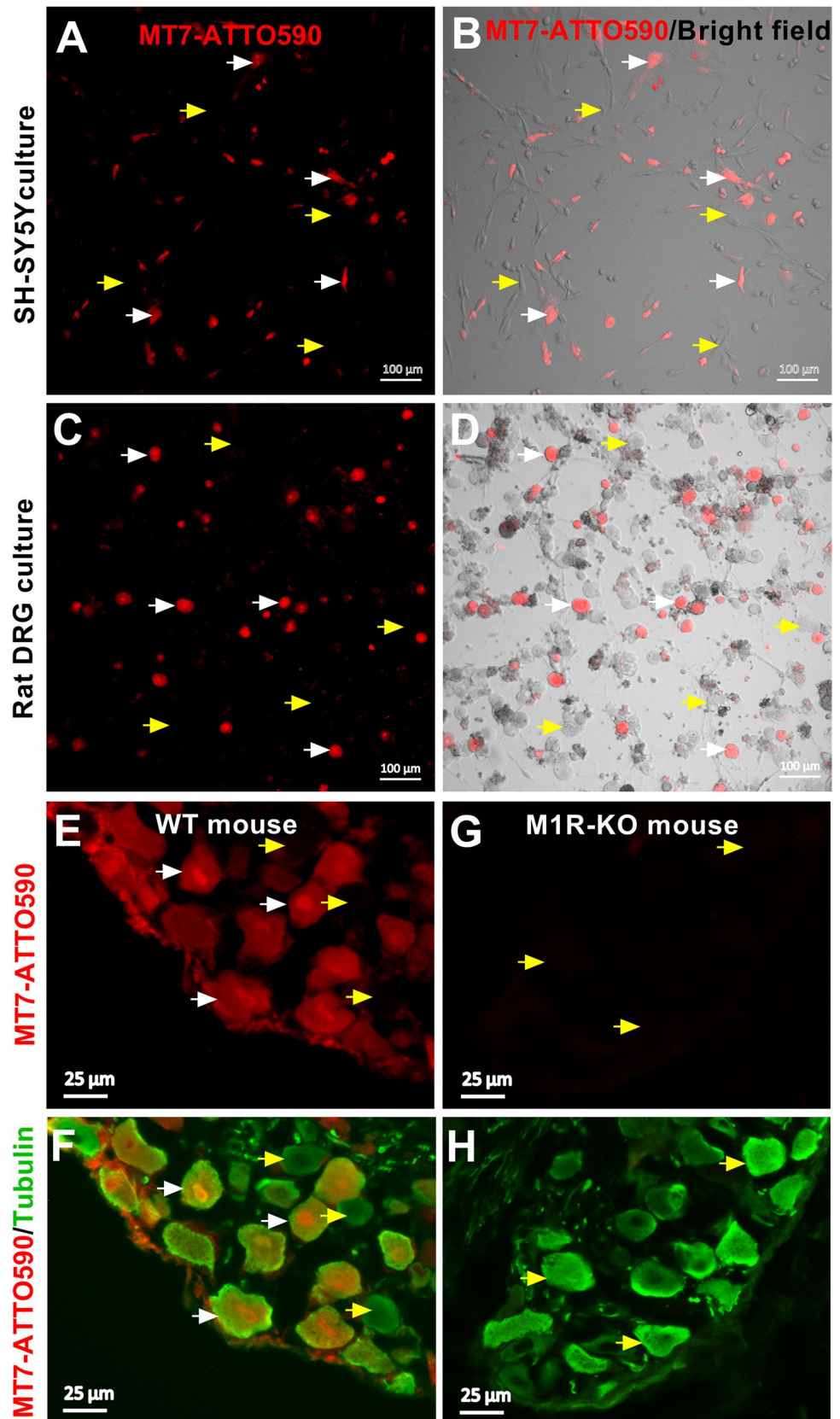
### Measurement of Mitochondrial Membrane Potential (MMP)

The MMP was evaluated by use of the fluorescent, lipophilic, and cationic probe, 5,5',6,6'-tetrachloro-1,1',3,3'-iodide (JC-1) (Invitrogen) according to the manufacturer's instructions. JC-1 dye stains mitochondria in a membrane potential-dependent manner. In functioning mitochondria with intact membrane potential differential, the mitochondria show a high red-to-green fluorescence ratio, whereas in depolarized mitochondria, the cationic dye is in monomeric form and produces a low red-to-green ratio [47]. The ratio of aggregate (red) to monomer (green) is decreased after the addition of FCCP (an uncoupler that dissipates the transmembrane electrochemical gradient). Cultured SH-SY5Y cells in 96-well plates (black clear-bottomed; Thermo Scientific) were loaded with 20 µM JC-1 and DRG neurons were loaded with 5 µM JC-1 staining solution for 15 min at 37 °C and washed with JC-1 staining buffer and then subjected to various treatments. The fluorescence intensity was measured by a Biotek Synergy Neo2 multimode plate reader with 485 nm for excitation and 530 nm for emission of green (monomer form) fluorescence, and 485 nm for excitation and 590 nm for emission for red (aggregate form) fluorescence. The MMP of cells in each group was evaluated as the fluorescence ratio of red to green. The data were expressed as the relative expression to the control.

### Assessment of Plasma Membrane Potential

Cultured DRG neurons or SH-SY5Y cells in 96-well plates (black clear-bottomed; Thermo Scientific) were loaded with 5 µM of DiBAC4(3) (Invitrogen) staining solution for 30 min at 37 °C to ensure dye distribution across the plasma membrane. DiBAC4(3) is an anionic potentiometric probe that partitions between cells and extracellular solution in a membrane potential-dependent manner [48]. With increasing membrane potential, the probe partitions into the cell, resulting in an increase in fluorescence due to dye interaction with intracellular lipids and proteins, whereas hyperpolarization evokes a decrease in fluorescence. Fluorescence signals were recorded (with a Carl Zeiss LSM510 confocal inverted microscope; excitation at 488 nm and emission 520 nm) for 8 min at 5 s intervals. After

**Fig. 1** Human neuroblastoma SH-SY5Y cell line and DRG neurons express M1 receptors. **A–D** Confocal images of cultured SH-SY5Y cells (**A, B**) and rat DRG neurons (**C, D**) stained with 100 nM MT7-ATTO590. **E–H** Immunohistochemistry images of mouse DRG tissues for wild type (**E, F**) and M<sub>1</sub>R KO (**G, H**) mice stained with 100 nM MT7-ATTO590. **F, H** Neuronal cells were stained with  $\beta$ -tubulin III antibodies. White arrows indicate M<sub>1</sub>R +ve and yellow arrows indicate M<sub>1</sub>R -ve cells or neurons. WT, wild type; M<sub>1</sub>R KO, M<sub>1</sub>R knock out



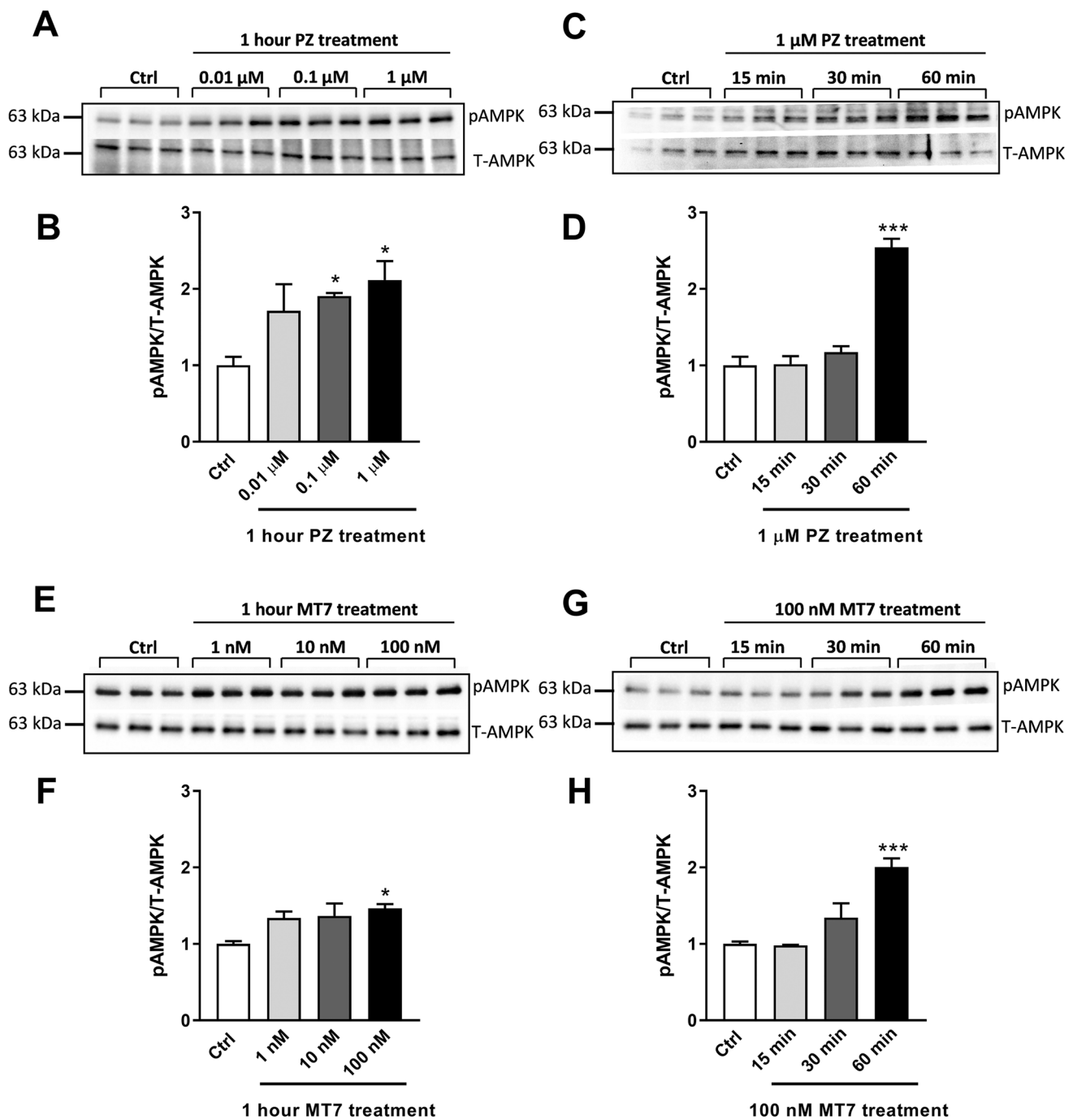


**Fig. 2** Pirenzepine and MT7 elevate phosphorylation of AMPK in a dose and time-dependent manner. **A** SH-SY5Y cells were cultured overnight, serum deprived (SD) for 4 h and then treated with various doses of pirenzepine (PZ) for 1 h. Western blots are shown for P-AMPK and T-AMPK. **B** Levels of expression of P-AMPK (in A) presented relative to T-AMPK. **C** SH-SY5Y cells were subjected to SD exposed to 1 μM PZ for various times (15 min, 30 min, and 60 min). **D** Levels of P-AMPK (in C) presented relative to T-AMPK. **E** SH-SY5Y cells were cultured overnight, starved for 4 h and then

treated with various doses of MT7 for 1 h. Western blots are shown for P-AMPK and T-AMPK. **F** Levels of expression of P-AMPK (in E) presented relative to T-AMPK. **G** SH-SY5Y cells were subjected to SD exposed to 100 nM MT7 for various times (15 min, 30 min, and 60 min). **H** Levels of P-AMPK (in G) presented relative to T-AMPK. Data are expressed as mean ± SEM,  $n = 3$  replicates; \* $p < 0.05$  and \*\*\* $p < 0.001$  vs control by one-way ANOVA with Dunnett's post hoc test

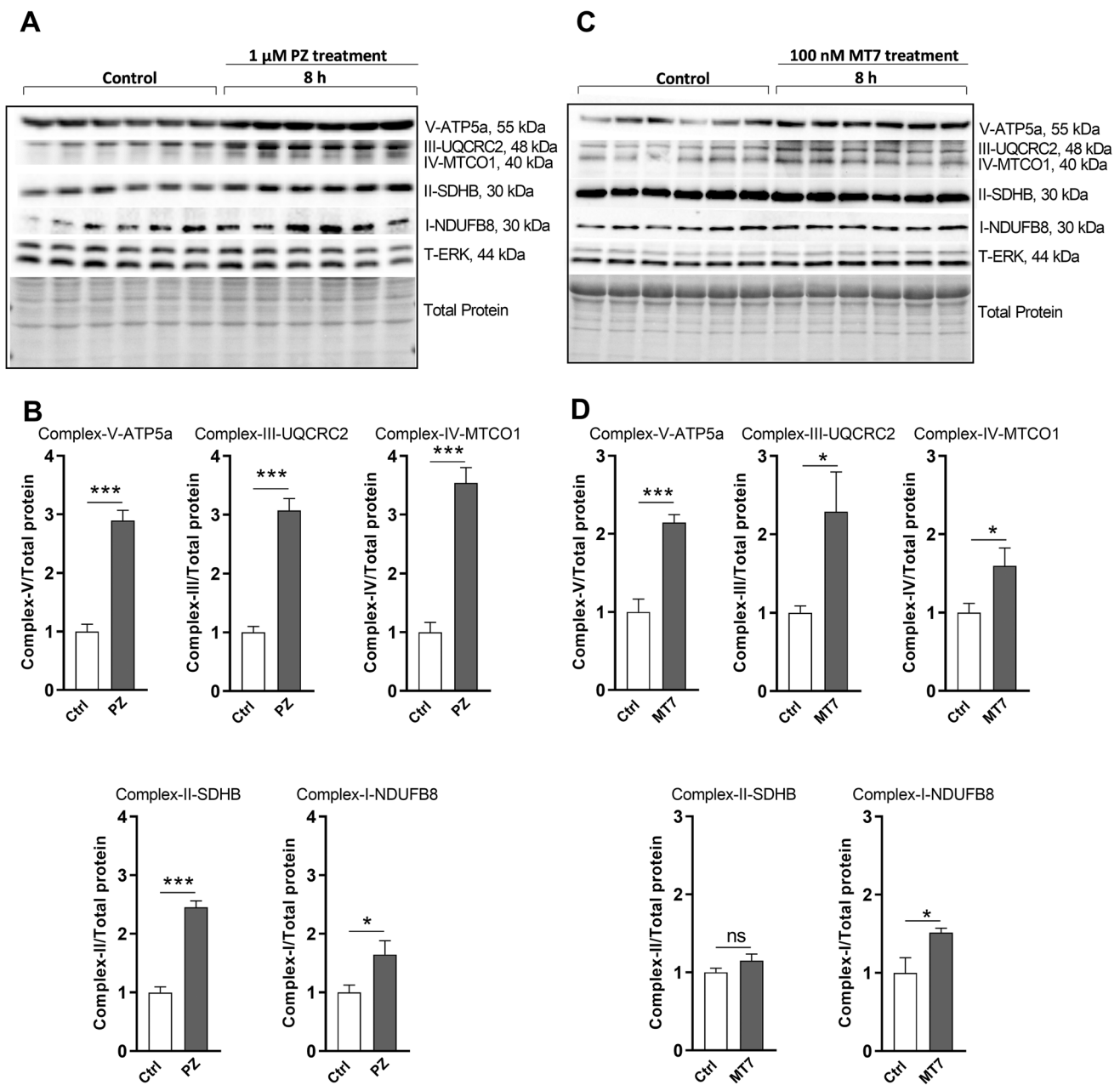


**Fig. 3** Pirenzepine and MT7 treatment increase the expression of mitochondrial respiratory chain proteins. **A–D** SH-SY5Y cells were treated with/without 1  $\mu\text{M}$  pirenzepine (PZ; **A, B**) and 100 nM MT7 (**C, D**) for 8 h, and lysates subjected to Western blotting. Representative Western blot (**A, C**) showing OXPHOS protein levels. Specific

measurement of 1 min basal fluorescence, drugs (MT7 100 nM, pirenzepine (PZ) 30  $\mu\text{M}$ , muscarine (Mus) 100  $\mu\text{M}$ ; prepared in the assay buffer containing DiBAC4(3)) were administered to the culture. At the end, 90 mM KCl was applied. Only neurons that responded to KCl with membrane depolarization were selected for analysis. Images were analyzed using Fiji software [49]. Regions of interest (ROIs) containing individual neurons were selected and fluorescence intensities quantified. Responses were corrected for any background changes in fluorescence and data were plotted with baseline correction.

proteins from each respiratory complex were quantified and expressed relative to total protein (**B, D**). Data are expressed as mean  $\pm$  SEM,  $n=6$  replicates; \* $p < 0.05$  or \*\* $p < 0.01$  or \*\*\* $p < 0.001$  vs control by unpaired Student's  $t$ -test

### Statistical Analysis

Data are expressed as mean  $\pm$  SEM, and where appropriate, data were subjected to unpaired 2-tailed Student's  $t$  test, one-way ANOVA with Tukey's, or Dunnett's multiple comparison post hoc tests. Area under the curve (AUC) analysis was performed using the trapezoidal rule with baseline correction. A value of  $p < 0.05$  was considered statistically significant. Graph-Pad Prism software was used to perform statistical analysis.

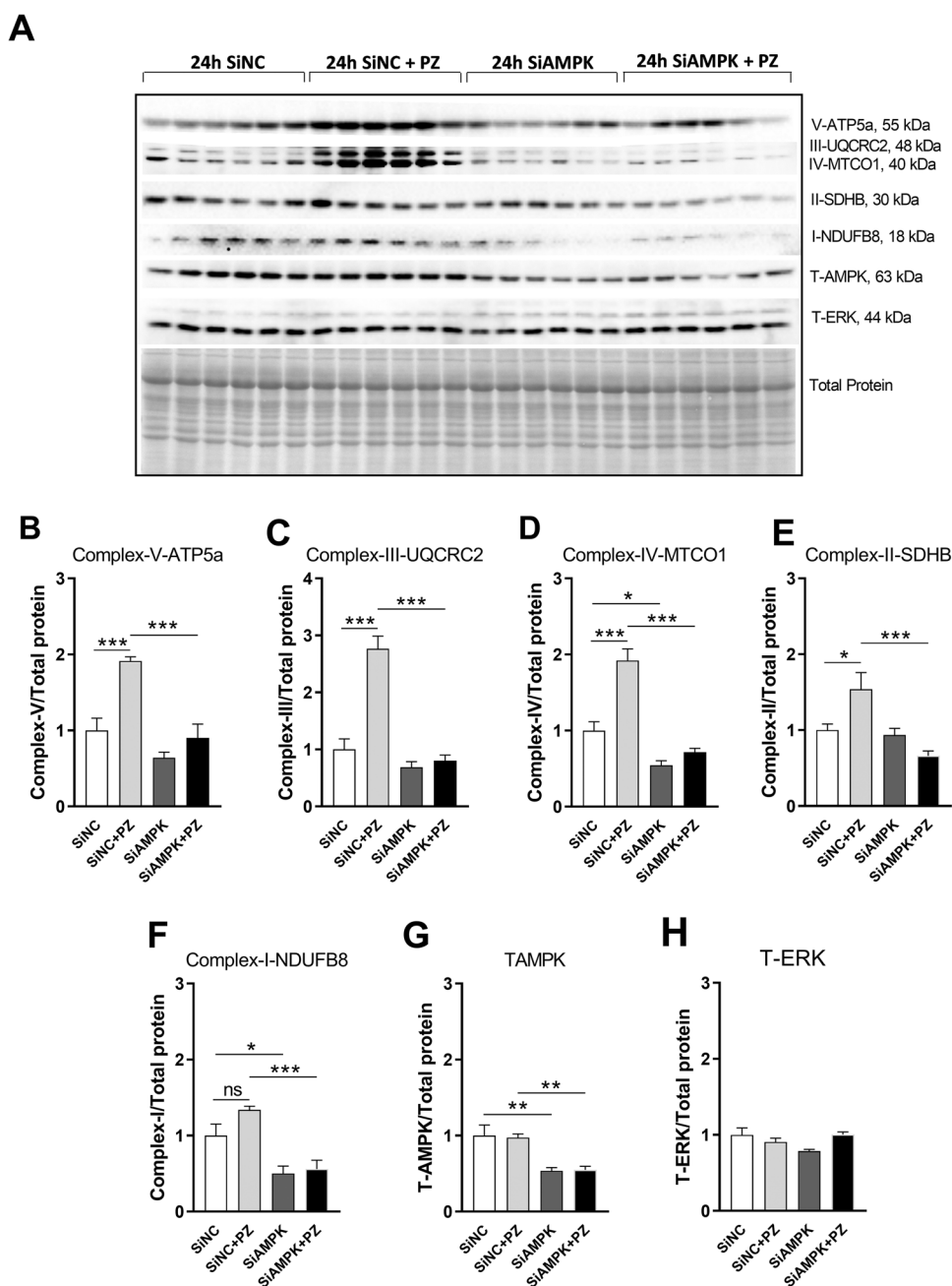
## Results

### Expression of M<sub>1</sub>R in Human Neuroblastoma SH-SY5Y Cell Line and Rodent DRG Neurons

The presence of M<sub>1</sub>R in SH-SY5Y cell line and rat DRG neurons was assessed by using MT7-ATTO590 (Fig. 1A–D). This labelled MT7 is absolutely specific for the M<sub>1</sub>R and is superior to the use of antibodies that cross-react with other MR sub-types. The specificity of MT7-ATTO590 was confirmed by using DRG tissues

from wild-type and M<sub>1</sub>R knock out (M<sub>1</sub>R KO) mice (Fig. 1E–H). The SH-SY5Y human neuroblastoma cell line is a well-characterized model to study muscarinic cholinergic function [50, 51] and we decided to use this cellular model to establish the effect of M<sub>1</sub>R antagonism. We also confirmed the mRNA expression levels of M<sub>1</sub>R in SH-SY5Y cells by using quantitative RT-PCR (Supplementary Fig. 1) and this data confirmed a previous report [52]. Overall, these observations clearly demonstrate that M<sub>1</sub>R is widely expressed in rodent DRG and neuroblastoma cells.

**Fig. 4** AMPK knockdown blocks pirenzepine-mediated upregulation of mitochondrial respiratory protein complexes. SH-SY5Y cells were cultured overnight, transfected with scrambled siRNA (siNC) or siRNAs specific to AMPK-isoforms  $\alpha 1$  and  $\alpha 2$  (siAMPK) and cultured for 24 h. Cells were subsequently treated with/without 1  $\mu$ M PZ for 8 h, and subjected to Western blotting. **A** Representative Western blot showing OXPHOS protein levels for control + siNC, PZ + siNC, control + siAMPK, and PZ + siAMPK. **B–G** Band intensity of each protein was normalized to total protein. Western blotting for total AMPK was used to calculate the knock-down efficiency of AMPK isoforms (A) where levels of expression of T-AMPK are presented relative to total protein (G). **H** Total ERK (T-ERK) was used as a loading control. Data are expressed as mean  $\pm$  SEM,  $n = 6$  replicates; \* $p < 0.05$  or \*\* $p < 0.01$  or \*\*\* $p < 0.001$  by one-way ANOVA with Tukey's post hoc test



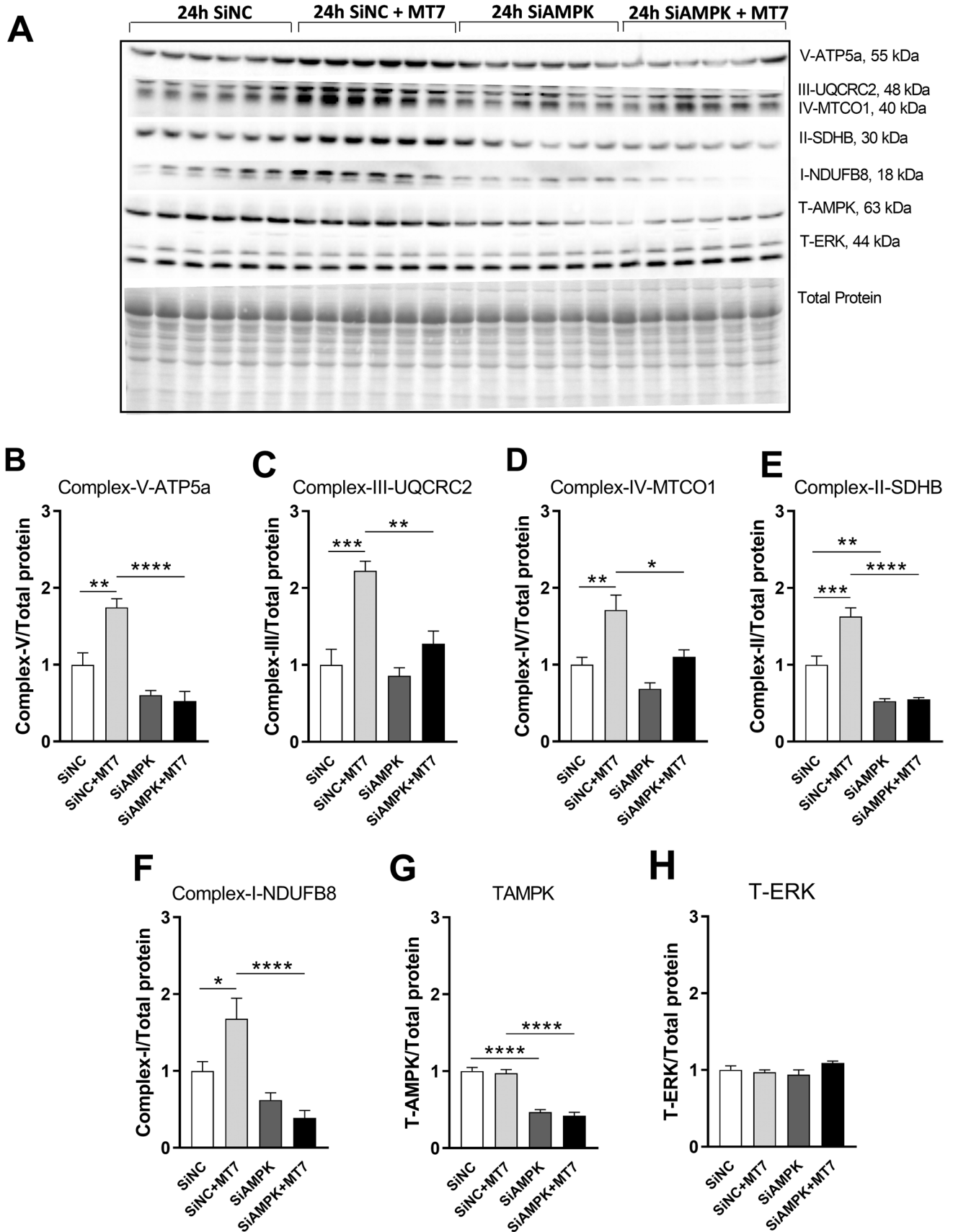




**Fig. 5** AMPK knockdown blocks MT7-dependent upregulation of mitochondrial respiratory protein complexes. SH-SY5Y cells were cultured overnight, transfected with scrambled siRNA (siNC) or siRNAs specific to AMPK-isoforms  $\alpha 1$  and  $\alpha 2$  (siAMPK) and cultured for 24 h. Cells were subsequently treated with/without 100 nM MT7 for 8 h, and subjected to Western blotting. **A** Representative Western blot showing OXPHOS protein levels for control+siNC, MT7+siNC, control+siAMPK, and MT7+siAMPK. **B–G** Band intensity of each protein was normalized to total protein. Western blotting for total AMPK was used to calculate the knockdown efficiency of AMPK isoforms (A) where levels of expression of T-AMPK are presented relative to total protein (G). **H** T-ERK was used as a loading control. Data are expressed as mean  $\pm$  SEM,  $n=6$  replicates; \* $p < 0.05$  or \*\* $p < 0.01$  or \*\*\* $p < 0.001$  by one-way ANOVA with Tukey's post hoc test

### Pirenzepine/MT7 Augment AMPK Phosphorylation in a Dose- and Time-Dependent Manner and Enhance Respiratory Chain Protein Expression and Mitochondrial Function in SH-SY5Y Cells

Pirenzepine- or MT7-induced AMPK activation was confirmed by detecting the phosphorylated form of AMPK (Fig. 2). SH-SY5Y cells were starved in serum free DMEM for 4 h before treatment. Western blots exhibited a marked dose-dependent and time-dependent elevation in AMPK phosphorylation (pAMPK) following pirenzepine/MT7 treatment. Quantification of pAMPK relative to T-AMPK revealed  $\sim 2.0$ -fold elevation at 1  $\mu$ M PZ (Fig. 2A, B) and  $\sim 1.5$ -fold elevation at 100 nM MT7 (Fig. 2E, F). A time course for the effect of 1  $\mu$ M pirenzepine and 100 nM MT7 was performed and revealed an elevation in pAMPK levels following 1 h of treatment, where pirenzepine caused a  $\sim 2.5$ -fold increase (Fig. 2C, D) and MT7 caused a  $\sim 2.0$ -fold enhancement in pAMPK (Fig. 2G, H). Previous studies reported that there are several downstream effectors of AMPK that contribute to the regulation of mitochondrial biogenesis [53, 54]. In line with these observations, pirenzepine/MT7 treatment (8 h, without starvation) induced mitochondrial OXPHOS proteins, components of the electron transport chain (ETC), including complex components V-ATP5a, III-UQCRC2, IV-MTCO1, II-SDHB, and I-NDUFB8 (Fig. 3A–D). In serum-deprived condition, 8 h treatment with pirenzepine or MT7 also exhibited enhanced mitochondrial protein expression (Supplementary Fig. 2), although some protein complexes were not statistically significant and changes not as robust as compared with the data (without starvation) revealed in Fig. 3. This may be explained by the fact that cells were subjected to increasing duration of serum deprivation and so experience a stressful condition [55]. In addition to mitochondrial protein expression, mitochondrial oxygen consumption rate (OCR) was enhanced with  $M_1R$  antagonist treatment (Supplementary Fig. 3). The bioenergetic parameter of maximal respiration was also

increased, although not reaching statistical significance ( $P < 0.06$ ) (Supplementary Fig. 3C). Relative ATP production, measured using the Seahorse machine, was augmented by MT7 treatment (Supplementary Fig. 3E). This confirms our previous work in cultured rat DRG neurons, and in tissues from STZ-induced diabetic rodents [29]), that blockade of  $M_1R$  enhances mitochondrial function.

### AMPK Knockdown Blocks Upregulation of Mitochondrial Respiratory Protein Complexes Driven by $M_1R$ Antagonists Pirenzepine and MT7 in SH-SY5Y Cells

Impaired AMPK signaling in DRG neurons is linked to mitochondrial dysfunction [24]. To confirm the causal involvement of AMPK activation in upregulation of mitochondrial protein complexes by pirenzepine/MT7, we employed siRNA-mediated AMPK knockdown in SH-SY5Y cells. Following 24 h of treatment with the siRNAs, the level of total-AMPK protein was significantly depleted (Figs. 4G and 5G). AMPK knockdown significantly blocked the upregulation of mitochondrial OXPHOS proteins induced by pirenzepine (Fig. 4A–F) or MT7 treatment (Fig. 5A–F).

### AMPK Inhibition or Downregulation Suppresses the Pirenzepine/MT7 Effect on Mitochondrial Membrane Potential (MMP) in SH-SY5Y Cells and Rat DRG Neurons

MMP generated by the proton pumps of the mitochondrial respiratory complexes is indispensable in the process of energy storage during oxidative phosphorylation [56]. MMP, a key indicator of cell health or injury, has become a useful parameter for monitoring changes in mitochondrial function [57]. Changes in MMP were analyzed by employing the mitochondrial cationic dye, JC-1 (Figs. 6 and 7). A time course experiment for the effect of 1  $\mu$ M pirenzepine was performed in SH-SY5Y cells. Exposure to pirenzepine for 6 h increased the MMP in SH-SY5Y cells (Fig. 6A). Similar time course experiment for 1  $\mu$ M pirenzepine and 100 nM MT7 was performed in cultured DRG neurons where MMP was elevated after 3 h of pirenzepine (Fig. 7A) or MT7 treatment (Fig. 7B). To see whether this upregulation was due to AMPK activation, SH-SY5Y cells and DRG neurons were treated with Compound C (a pharmacological AMPK inhibitor) or transfected with siRNAs to AMPK. Pharmacological blockade of AMPK using Compound C suppressed the pirenzepine (Fig. 6B) or MT7 (Fig. 7C) induced elevation of MMP. siRNA-based inhibition of AMPK also exhibited a similar suppression of pirenzepine-induced enhancement of MMP in SH-SY5Y cells (Fig. 6C).

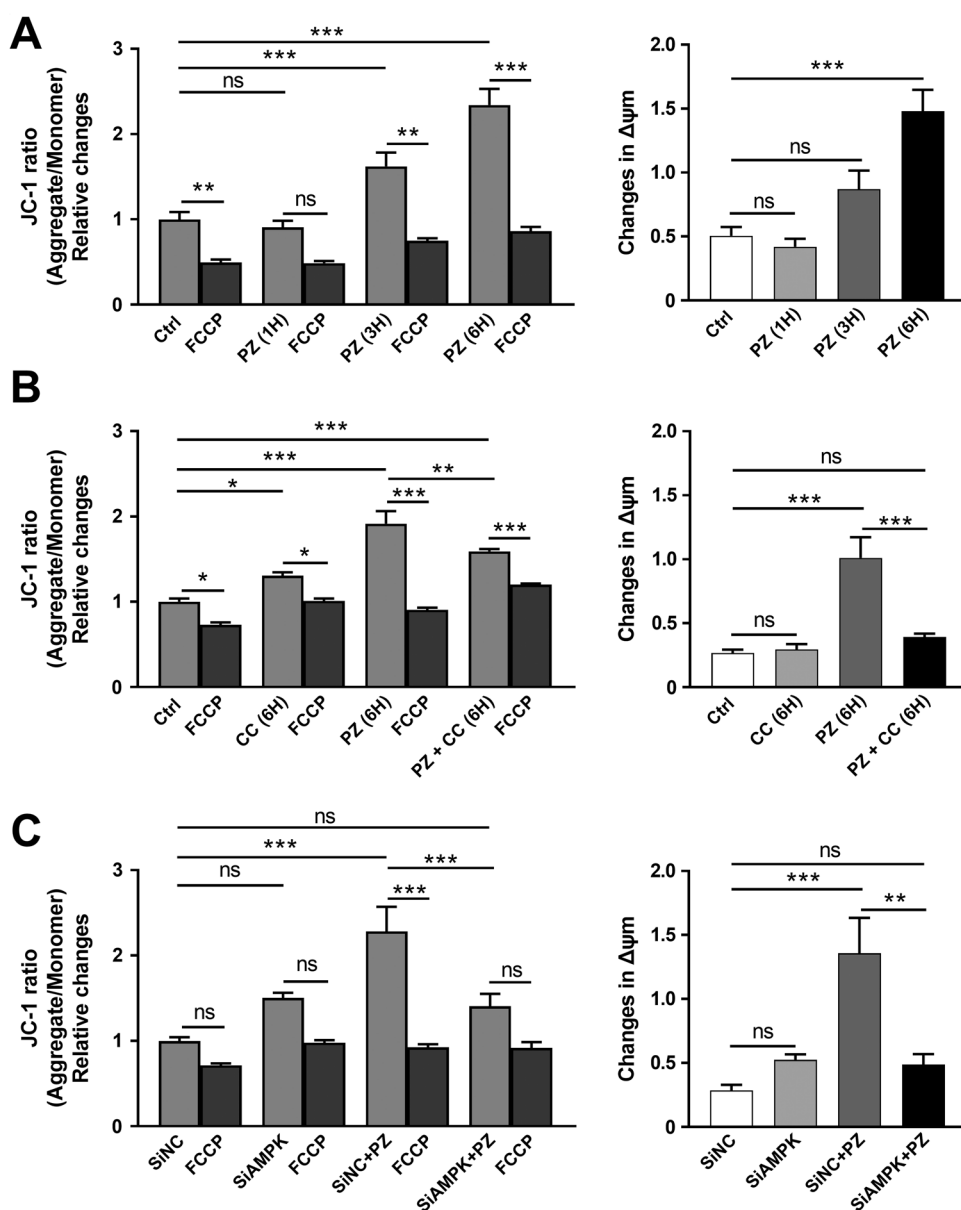
## Role of M<sub>1</sub>R Antagonists in the Regulation of Plasma Membrane Potential in Primary DRG Neurons and SH-SY5Y Cells

Cultured DRG neurons were loaded with the voltage sensor probe DiBAC4(3) to evaluate the plasma membrane potential (V<sub>m</sub>). In DRG neurons, M<sub>1</sub>R antagonists (MT7 or pirenzepine) induced hyperpolarization thus inducing a less excitable state. The muscarinic receptor agonist, muscarine, depolarized the neuronal plasma membrane potential (Fig. 8A–J). The same experiment was performed in SH-SY5Y cells where there was a similar hyperpolarizing response to MT7 and depolarization to muscarine (Supplementary Fig. 4A–F).

## Discussion

The findings in our current study indicate a link between impaired AMPK signaling and mitochondrial respiratory chain dysfunction in human neuroblastoma SH-SY5Y cells. The SH-SY5Y cell line has been used extensively as an in vitro model system of peripheral sensory neurons as they exhibit traits of sensory neuron phenotype [58]. Thus, the rationale for this approach is that the assay performed in this cell line can be a predictor of efficacy in human cells and will be useful for future drug screening endeavors [59]. In addition, this work provides important background information that will underpin future molecular studies not feasible in primary neurons, e.g., proteomic studies to understand

**Fig. 6** Effects of pirenzepine treatment on mitochondrial membrane potential in SH-SY5Y cells. SH-SY5Y cells were cultured overnight, stained with JC-1 dye to analyze mitochondrial membrane potential (MMP) and subsequently, the loss of MMP in response to FCCP. **A** Cells were treated with/without 1  $\mu$ M pirenzepine (PZ) for various times (1 h, 3 h, and 6 h). **B** Cells were treated with AMPK inhibitor compound C (CC, 3  $\mu$ M) with/without 1  $\mu$ M PZ for 6 h. **C** SH-SY5Y cells were cultured overnight, transfected with scrambled siRNA (siNC) and siRNAs specific to AMPK-isoforms  $\alpha$ 1 and  $\alpha$ 2 (siAMPK) and were cultured for 24 h. Cells were subsequently treated with/without 1  $\mu$ M PZ for 6 h. Fluorescence ratio was used for MMP quantitative analysis. The ratio of aggregate to monomer is decreased after the addition of FCCP (an uncoupler). All the left panels show the MMP, whereas the right panels show changes in MMP after FCCP treatment. The JC-1 dye ratio was determined using a Biotek Neo2 Synergy multimode plate reader. Data are expressed as mean  $\pm$  SEM,  $n = 10$ –15 replicates; \* $p < 0.05$  or \*\* $p < 0.01$  or \*\*\* $p < 0.001$  by one-way ANOVA with Tukey's post hoc test

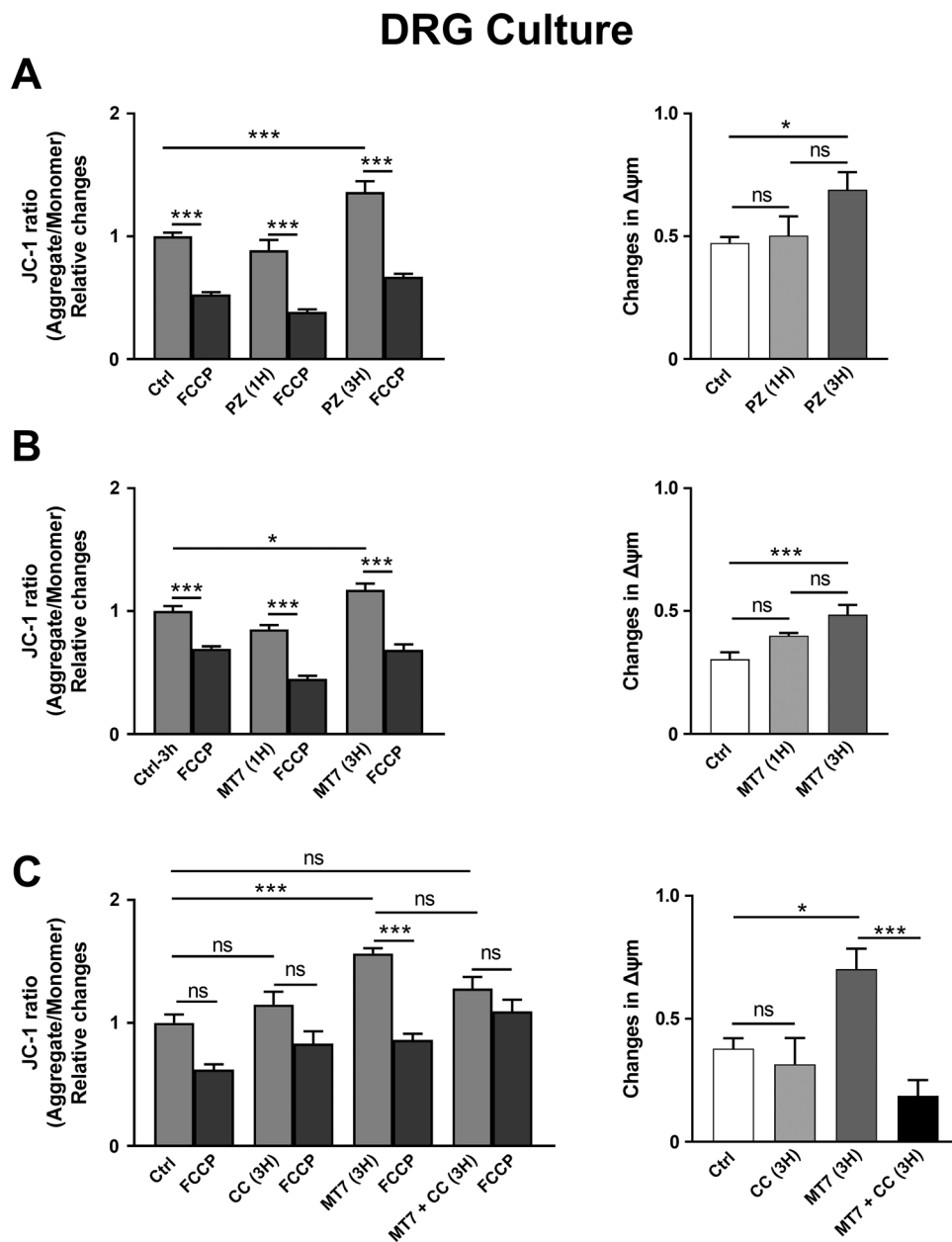


molecular pharmacology at the  $M_1R$  (for example, see [60]). We observed MT7 and pirenzepine treatment enhanced AMPK phosphorylation, augmented mitochondrial complex protein expression, and enhanced mitochondrial function in the SH-SY5Y cell line, and these data support our previous report in DRG neurons [23, 24, 29, 30]. Importantly, siRNA targeting AMPK significantly blocked the drug-induced upregulation of mitochondrial OXPHOS proteins resulting in a suppressed oxidative phosphorylation system.

Dynamic morphological changes in mitochondria are required to maintain a homogenous population of functional mitochondria to ensure continuous and optimal mitochondrial respiration. Optimal mitochondrial function is a key factor for axonal outgrowth and repair [37, 61].

Mitochondrial abnormalities have been proposed to mediate development of diabetic complications through cellular dysfunction in endothelial cells, skeletal muscle, cardiomyocytes, and neurons [23, 24, 26, 62–64]. Mitochondrial biogenesis is triggered by the AMPK-PGC-1 $\alpha$ -Nrf1 pathway which, in turn, regulates the expression of both mitochondrial and nuclear genes encoding respiratory chain subunits and other proteins that are required for mitochondrial function [65, 66]. Energy supplementation provided by this pathway is required for axonal outgrowth and neuronal growth [65]. Previous studies have highlighted that activation of AMPK can elevate neurite outgrowth. For example, resveratrol, an activator of AMPK, drives axonal outgrowth and was protective against diabetic neuropathy in STZ-induced

**Fig. 7** Effects of pirenzepine and MT7 treatment on MMP in DRG neurons. DRG neurons derived from adult control rats were cultured for 24 h, stained with JC-1 dye to evaluate MMP and the loss of MMP subsequent to FCCP application. **A**, **B** Neurons were treated with/without 1  $\mu$ M PZ (A) or 100 nM MT7 (B) for various times (1 h and 3 h). **C** Neurons were treated with AMPK inhibitor compound C (CC, 3  $\mu$ M) with/without 100 nM MT7 for 3 h. All the left panels show the MMP, whereas the right panels show changes in MMP after FCCP treatment. Data are expressed as mean  $\pm$  SEM,  $n=8-10$  replicates; \* $p<0.05$  or \*\* $p<0.01$  or \*\*\* $p<0.001$  by one-way ANOVA with Tukey's post hoc test



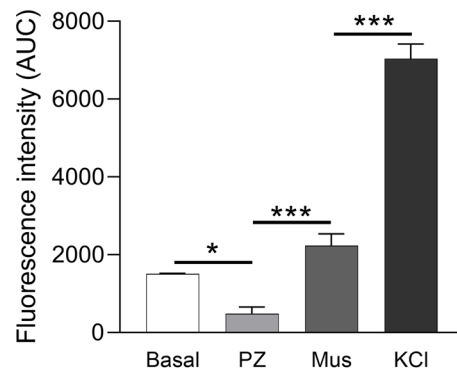
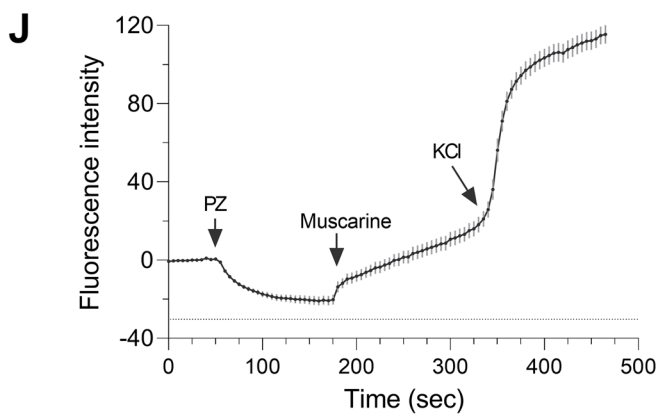
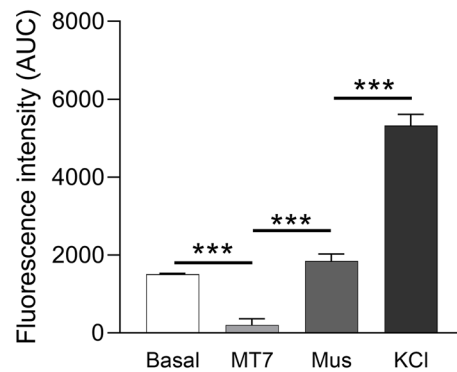
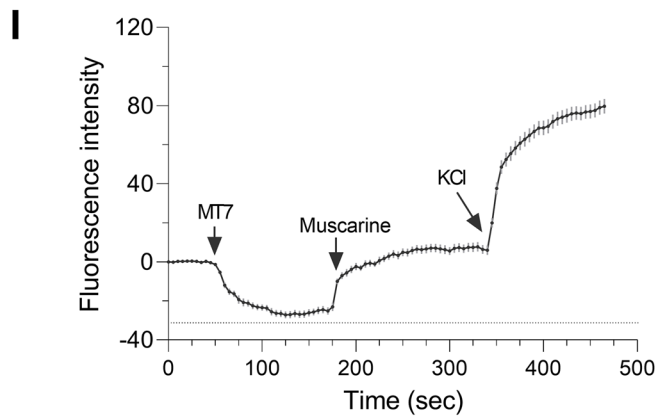
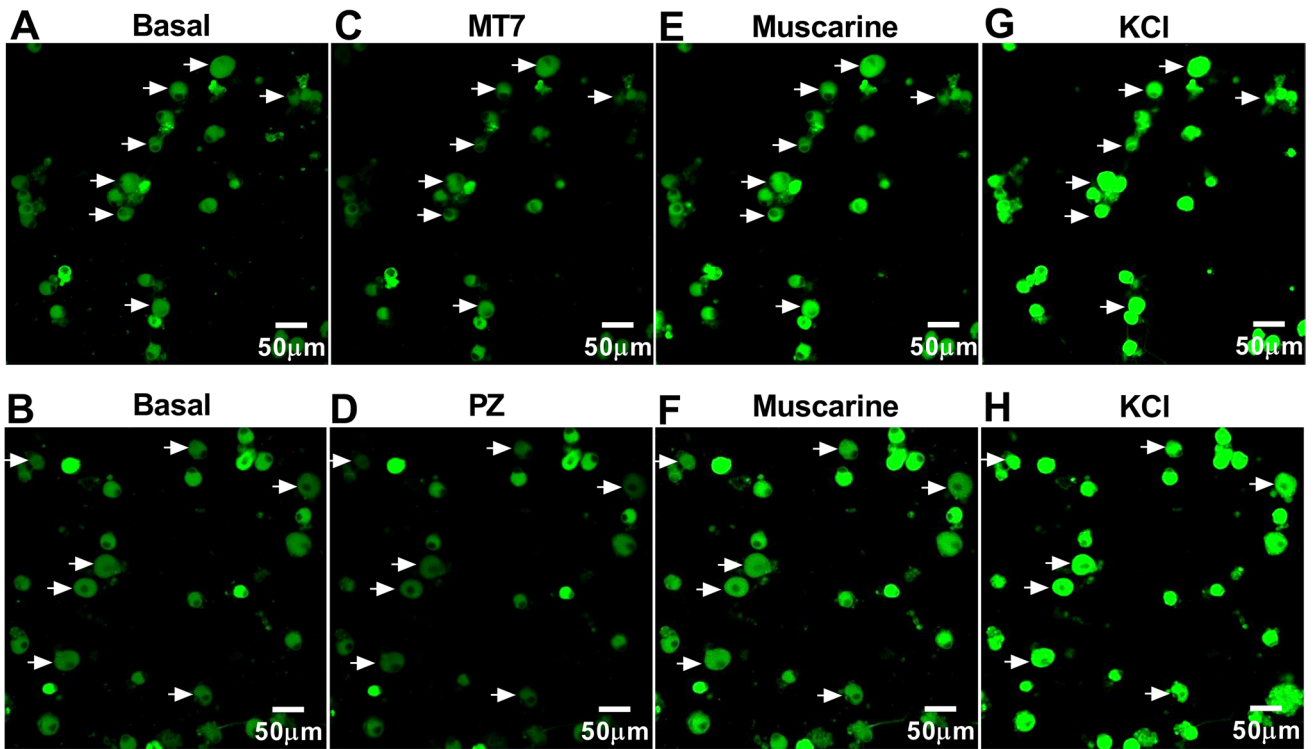


**Fig. 8** Changes in the plasma membrane potential in response to  $M_1R$  antagonists or agonist in DRG neurons. **A–H.** Confocal images of primary cultures of DRG neurons in the presence of the resting membrane potential probe DiBAC4(3) showing fluorescence at basal (A, B) and after administration of 100 nM MT7 (C), 30  $\mu$ M PZ (D), 100  $\mu$ M muscarine (Mus; E, F), and 90 mM KCl (G, H). Arrows indicate a selection of neurons that responded to MT7 or PZ. **I–J.** Traces of DiBAC4(3) fluorescence intensity (left panel) and AUC (right panel) show the changes in plasma membrane potential measured in response to MT7 (I) or PZ (J) followed by muscarine and KCl. The AUC was estimated for 1 min before each treatment (MT7/PZ, Mus, KCl) from the baseline to a relative fluorescence level of  $-30$ . Data are expressed as mean  $\pm$  SEM,  $n = 50$ – $54$  neurons;  $*p < 0.05$  or  $**p < 0.01$  or  $***p < 0.001$  by one-way ANOVA with Tukey's post hoc test

diabetic rats [24, 67]. Recent studies also report IGF-1-mediated upregulation of mitochondrial respiration together with a dose-dependent stimulation of ATP production through AMPK in a type 1 model of diabetes [36]. Other works have determined that certain mitochondrial complexes and mitochondrial membrane potential were impaired in cortical tissues and primary DRG neurons from diabetic rat but the cellular mechanisms are not completely understood [23, 25, 68].

The present study demonstrates for the first time that blockade of the  $M_1R$  by the specific antagonist MT7 or the selective antagonist pirenzepine causes an augmentation of the mitochondrial membrane potential (MMP) in both cultured SH-SY5Y cells and DRG neurons. This stimulatory effect on MMP was time dependent and triggered within 1 h. MMP is a parameter for mitochondrial metabolic state and provides an estimate of the ATP production within individual mitochondria [69]. The AMPK inhibitor, Compound C, abolished the pirenzepine and MT7-mediated upregulation of mitochondrial MMP. SiRNA-based inhibition of endogenous AMPK exhibited a similar suppression of the pirenzepine enhancement of MMP. These novel observations in neurons provide functional evidence linking AMPK and alterations in mitochondrial performance, such as maintenance of MMP.

$M_1R$  activation inhibits voltage-gated Kv7 potassium channels that mediate the M-current in sympathetic neurons [43, 70]. M-current ( $I_M$ ) is a low-threshold, slowly activating potassium current in sympathetic neurons where it functions as a “brake” for neurons receiving persistent excitatory input [70]. The M-current is strongly suppressed by  $M_1R$  activation [42, 45, 71, 72] which is known to play an important role in modulating neuronal excitability and its suppression is predicted to increase input resistance in response to excitatory synaptic inputs [70, 73–75]. M-current inhibition via  $M_1R$  activation by acetylcholine is phosphatidylinositol-4,5-bisphosphate ( $PIP_2$ )-dependent with depletion of  $PIP_2$  dramatically decreasing Kv7 channel open probability [76, 77]. Acute ACh activation of  $M_1R$  promotes  $PIP_2$  hydrolysis

through phospholipase C activation, resulting in PKC phosphorylation and generation of inositol triphosphate, which induces endoplasmic reticulum  $Ca^{2+}$  release [78]. Downstream  $Ca^{2+}$ -dependent pathways drive closing of Kv7 channels, and the outcome is an enhanced propensity for depolarization of the plasma membrane. Interestingly, activated PKC may also contribute to the muscarinic inhibition of Kv7 channels [79]. Activated PKC phosphorylates the C-terminus in the calmodulin (CaM) binding site of the Kv7.2 subunit assisted by A-kinase-anchoring protein AKAP79/150. The phosphorylated state of the channel destabilizes the Kv7 channel/ $PIP_2$  complex and consequently  $PIP_2$  hydrolysis suppresses the M-current [80–83].

Kv7/M-channel activity represents an integral regulator of PNS sensitivity downstream of multiple transduction mechanisms likely to contribute to dampening of peripheral pain pathways [84]. They are densely expressed at the sites of spike generation, e.g., axon initial segment of central neurons and terminals of peripheral nociceptive neurons [85, 86]. Previous investigations of the role of Kv7 in regulating neuronal excitability, pain pathways, and nociceptive behaviors utilized pharmacological M-channel blockers or enhancers [41, 87–90]. M-current perturbations were strongly implicated in neuronal hyperexcitability underlying epilepsy and ALS [87, 91], neuroinflammation [92], and neuropathic pain [93, 94]. M-current “opener” compounds have been suggested to be efficacious in preventing brain damage after multiple types of insults/diseases, such as stroke, traumatic brain injury, drug addiction, and mood disorders [95]. However, sensory neurons express Kv7 channels and exhibit the M-current, activated at near resting potential such that at subthreshold potentials produce a prominent outward current [41, 42, 96] helping to keep the resting potential within a hyperpolarized range but an initiating role of  $M_1R$  in this pathway has not been directly elucidated [41, 97]. In accordance with this concept, the present experiments revealed that antimuscarinic drugs pirenzepine or MT7 have a novel mechanism of action acting as putative positive modulators of Kv7 M-channels, i.e., Kv7 channel opener/enhancers in SH-SY5Y cells and sensory neurons. Consequently,  $M_1R$  antagonists help to establish the neuronal resting membrane potential by providing a continual hyperpolarizing influence and make the neurons less excitable. The effects of pirenzepine/MT7 on M-current activation were reversed by muscarinic agonist muscarine leading to increased responsiveness of neurons toward depolarizing stimuli.

As such, the data presented here offer promising evidence for the pivotal role of the Kv7 channel as a target of  $M_1R$  antagonists to stabilize membrane potential as well as dampening deviations in depolarization and, therefore, preventing ectopic firing and spontaneous pain. Importantly, upon axotomy, sensory neurons exhibit spontaneous electrical activity that consumes extensive ATP [98–101].  $M_1R$  antagonism enhances

neurite outgrowth of axotomized adult sensory neurons in culture. Therefore, enhancement of the M-current would reduce the possibility of depolarization, thus theoretically preserving ATP to support actin treadmilling in the growth cone and enhancing axon outgrowth [29, 102]. Thus, pirenzepine and MT7 could be signaling via two self-supporting but different pathways to drive axon outgrowth: the AMPK pathway, which is dependent upon a drug-induced rise in intracellular  $\text{Ca}^{2+}$  and activation of CaMKK $\beta$  [29, 30], and a supplementary pathway involving antimuscarinic elevation of the M-current and hyperpolarization of the plasma membrane and conservation of ATP levels. This latter pathway would be expected to downregulate AMPK activity; however, we propose the drug-induced  $\text{Ca}^{2+}$  influx overrides this effect. At this stage, we have no evidence that antimuscarinic drug action, possibly mediated through the opening of Kv7 channels, has any role in AMPK activation. However, recent work localizing functional Kv7.4 channels to the mitochondria of cardiac myocytes and CNS neurons provides an intriguing link between the M-current and regulation of cellular bioenergetics and is worthy of future investigation in adult sensory neurons [103].

## Conclusions

Our present findings highlight the utility of muscarinic receptor antagonism as a tool to manipulate the AMPK pathway which is a central component of the pathogenic cascade linking mitochondrial function with neurodegeneration. We have demonstrated that pirenzepine or MT7 enhances mitochondrial function via AMPK and regulate mitochondrial membrane potential and the plasma membrane potential. Pirenzepine or MT7 enhances the M-current activity that is crucially important for controlling the excitability of neurons. Thus, these findings strengthen the case for using M $_1$ R antagonists for improvement of mitochondrial function, while the ability to suppress excitability of sensory neurons may offer routes for treatment of neuropathic pain as well as simultaneously promoting nerve regeneration in neurodegenerative diseases.

**Supplementary Information** The online version contains supplementary material available at <https://doi.org/10.1007/s12035-022-03003-1>.

**Acknowledgements** We are grateful to St Boniface Hospital Research for continued support. We thank Dr. Jun-Feng Wang, University of Manitoba, for the gift of the human neuroblastoma SH-SY5Y cell line.

**Author Contribution** F.N. performed all experiments and wrote the first version of the manuscript. T.M.Z.W. validated and performed the staining using labelled MT7. P.F. obtained funding for the work, designed the experimental plan and edited and finalized the manuscript.

**Funding** This work was supported by grant # PJT-162172 from the Canadian Institutes of Health Research to P.F. F.N. was supported by a MITACs Accelerate postdoctoral training award where WinSanTor Inc provided matching funds (Project # IT14860).

**Data Availability** The datasets used and/or analyzed during the current study are available from the corresponding author on reasonable request.

## Declarations

**Ethics Approval and Consent to Participate** All animal protocols carefully followed Canadian Committee on Animal Care (CCAC).

**Consent for Publication** Not applicable.

**Competing Interests** The corresponding author, P.F., declares he is a co-founder and shareholder in WinSanTor Inc., which has licensed IP from the University of Manitoba.

**Open Access** This article is licensed under a Creative Commons Attribution 4.0 International License, which permits use, sharing, adaptation, distribution and reproduction in any medium or format, as long as you give appropriate credit to the original author(s) and the source, provide a link to the Creative Commons licence, and indicate if changes were made. The images or other third party material in this article are included in the article's Creative Commons licence, unless indicated otherwise in a credit line to the material. If material is not included in the article's Creative Commons licence and your intended use is not permitted by statutory regulation or exceeds the permitted use, you will need to obtain permission directly from the copyright holder. To view a copy of this licence, visit <http://creativecommons.org/licenses/by/4.0/>.

## References

1. Kruse AC, Kobilka BK, Gautam D, Sexton PM, Christopoulos A, Wess J (2014) Muscarinic acetylcholine receptors: novel opportunities for drug development. *Nat Rev Drug Discov* 13(7):549–560. <https://doi.org/10.1038/nrd4295>
2. Bonner TI (1989) New subtypes of muscarinic acetylcholine receptors. *Trends Pharmacol Sci Suppl*:11–15
3. Liu J, Blin N, Conklin BR, Wess J (1996) Molecular mechanisms involved in muscarinic acetylcholine receptor-mediated G protein activation studied by insertion mutagenesis. *J Biol Chem* 271(11):6172–6178. <https://doi.org/10.1074/jbc.271.11.6172>
4. Wess J (1996) Molecular biology of muscarinic acetylcholine receptors. *Crit Rev Neurobiol* 10(1):69–99. <https://doi.org/10.1615/critrevneurobiol.v10.i1.40>
5. Wess J, Eglén RM, Gautam D (2007) Muscarinic acetylcholine receptors: mutant mice provide new insights for drug development. *Nat Rev Drug Discov* 6(9):721–733. <https://doi.org/10.1038/nrd2379>
6. Kruse AC, Weiss DR, Rossi M, Hu J, Hu K, Eitel K, Gmeiner P, Wess J et al (2013) Muscarinic receptors as model targets and antitargets for structure-based ligand discovery. *Mol Pharmacol* 84(4):528–540. <https://doi.org/10.1124/mol.113.087551>
7. Thal DM, Sun B, Feng D, Nawaratne V, Leach K, Felder CC, Bures MG, Evans DA et al (2016) Crystal structures of the M1 and M4 muscarinic acetylcholine receptors. *Nature* 531(7594):335–340. <https://doi.org/10.1038/nature17188>

8. Birdsall NJ, Hulme EC, Stockton J, Burgen AS, Berrie CP, Hammer R, Wong EH, Zigmond MJ (1983) Muscarinic receptor subclasses: evidence from binding studies. *Adv Biochem Psychopharmacol* 37:323–329
9. Maeda M, Tsuda M, Tozaki-Saitoh H, Inoue K, Kiyama H (2010) Nerve injury-activated microglia engulf myelinated axons in a P2Y12 signaling-dependent manner in the dorsal horn. *Glia* 58(15):1838–1846. <https://doi.org/10.1002/glia.21053>
10. Max SI, Liang JS, Potter LT (1993) Purification and properties of m1-toxin, a specific antagonist of m1 muscarinic receptors. *J Neurosci* 13(10):4293–4300. <https://doi.org/10.1523/jneurosci.13-10-04293.1993>
11. Mironov SL (2007) ADP regulates movements of mitochondria in neurons. *Biophys J* 92(8):2944–2952. <https://doi.org/10.1529/biophysj.106.092981>
12. Chen H, Chan DC (2006) Critical dependence of neurons on mitochondrial dynamics. *Curr Opin Cell Biol* 18(4):453–459. <https://doi.org/10.1016/j.ceb.2006.06.004>
13. Kruger L, Perl ER, Sedivec MJ (1981) Fine structure of myelinated mechanical nociceptor endings in cat hairy skin. *J Comp Neurol* 198(1):137–154. <https://doi.org/10.1002/cne.901980112>
14. Ribeiro-da-Silva A, Kenigsberg RL, Cuello AC (1991) Light and electron microscopic distribution of nerve growth factor receptor-like immunoreactivity in the skin of the rat lower lip. *Neuroscience* 43(2–3):631–646. [https://doi.org/10.1016/0306-4522\(91\)90322-f](https://doi.org/10.1016/0306-4522(91)90322-f)
15. Zhang J, Ney PA (2010) Reticulocyte mitophagy: monitoring mitochondrial clearance in a mammalian model. *Autophagy* 6(3):405–408. <https://doi.org/10.4161/auto.6.3.11245>
16. Kim I, Lemasters JJ (2011) Mitophagy selectively degrades individual damaged mitochondria after photoirradiation. *Antioxid Redox Signal* 14(10):1919–1928. <https://doi.org/10.1089/ars.2010.3768>
17. Garrido-Maraver J, Paz MV, Cordero MD, Bautista-Lorite J, Oropesa-Ávila M, de la Mata M, Pavón AD, de Laveria I et al (1852) Sánchez-Alcázar JA (2015) Critical role of AMP-activated protein kinase in the balance between mitophagy and mitochondrial biogenesis in MELAS disease. *Biochim Biophys Acta* 11:2535–2553. <https://doi.org/10.1016/j.bbdis.2015.08.027>
18. Lv P, Zhu X, Wang J, Li G, Shen XY, Ke J, Wang C, Xiong S (2020) Experimental study of Shenfu injection on the prevention and treatment of paclitaxel chemotherapy DRG neuron injury. *Evid Based Complement Alternat Med* 2020:8239650. <https://doi.org/10.1155/2020/8239650>
19. Raha S, Robinson BH (2000) Mitochondria, oxygen free radicals, disease and ageing. *Trends Biochem Sci* 25(10):502–508. [https://doi.org/10.1016/s0968-0004\(00\)01674-1](https://doi.org/10.1016/s0968-0004(00)01674-1)
20. Liu Y, Qiukai E, Zuo J, Tao Y, Liu W (2013) Protective effect of Cordyceps polysaccharide on hydrogen peroxide-induced mitochondrial dysfunction in HL-7702 cells. *Mol Med Rep* 7(3):747–754. <https://doi.org/10.3892/mmr.2012.1248>
21. Kalvelytė AV, Imbrasaitė A, Krestnikova N, Stulpinas A (2017) Adult stem cells and anticancer therapy. In: Fishbein JC, Heilman JM (eds) *Advances in molecular toxicology*, vol 11. Elsevier, pp 123–202. <https://doi.org/10.1016/B978-0-12-812522-9.00004-X>
22. Mathur A, Hong Y, Kemp BK, Barrientos AA, Erusalimsky JD (2000) Evaluation of fluorescent dyes for the detection of mitochondrial membrane potential changes in cultured cardiomyocytes. *Cardiovasc Res* 46(1):126–138. [https://doi.org/10.1016/s0008-6363\(00\)00002-x](https://doi.org/10.1016/s0008-6363(00)00002-x)
23. Akude E, Zherebitskaya E, Chowdhury SK, Smith DR, Dobrowsky RT, Fernyhough P (2011) Diminished superoxide generation is associated with respiratory chain dysfunction and changes in the mitochondrial proteome of sensory neurons from diabetic rats. *Diabetes* 60(1):288–297. <https://doi.org/10.2337/db10-0818>
24. Roy Chowdhury SK, Smith DR, Saleh A, Schapansky J, Marquez A, Gomes S, Akude E, Morrow D et al (2012) Impaired adenosine monophosphate-activated protein kinase signalling in dorsal root ganglia neurons is linked to mitochondrial dysfunction and peripheral neuropathy in diabetes. *Brain* 135(Pt 6):1751–1766. <https://doi.org/10.1093/brain/aws097>
25. Srinivasan S, Stevens M, Wiley JW (2000) Diabetic peripheral neuropathy: evidence for apoptosis and associated mitochondrial dysfunction. *Diabetes* 49(11):1932–1938. <https://doi.org/10.2337/diabetes.49.11.1932>
26. Chowdhury SK, Zherebitskaya E, Smith DR, Akude E, Chattopadhyay S, Jolivald CG, Calcutt NA, Fernyhough P (2010) Mitochondrial respiratory chain dysfunction in dorsal root ganglia of streptozotocin-induced diabetic rats and its correction by insulin treatment. *Diabetes* 59(4):1082–1091. <https://doi.org/10.2337/db09-1299>
27. Urban MJ, Pan P, Farmer KL, Zhao H, Blagg BS, Dobrowsky RT (2012) Modulating molecular chaperones improves sensory fiber recovery and mitochondrial function in diabetic peripheral neuropathy. *Exp Neurol* 235(1):388–396. <https://doi.org/10.1016/j.expneurol.2012.03.005>
28. Chandrasekaran K, Anjaneyulu M, Choi J, Kumar P, Salimian M, Ho CY, Russell JW (2019) Role of mitochondria in diabetic peripheral neuropathy: influencing the NAD(+)-dependent SIRT1-PGC-1 $\alpha$ -TFAM pathway. *Int Rev Neurobiol* 145:177–209. <https://doi.org/10.1016/bs.irn.2019.04.002>
29. Calcutt NA, Smith DR, Frizzi K, Sabbir MG, Chowdhury SK, Mixcoatl-Zecuatl T, Saleh A, Muttalib N et al (2017) Selective antagonism of muscarinic receptors is neuroprotective in peripheral neuropathy. *J Clin Invest* 127(2):608–622. <https://doi.org/10.1172/JCI88321>
30. Saleh A, Sabbir MG, Aghanoori MR, Smith DR, Roy Chowdhury SK, Tessler L, Brown J, Gedarevich E et al (2020) Muscarinic toxin 7 signals via Ca(2+)/calmodulin-dependent protein kinase  $\beta$  to augment mitochondrial function and prevent neurodegeneration. *Mol Neurobiol* 57(6):2521–2538. <https://doi.org/10.1007/s12035-020-01900-x>
31. Feige JN, Auwerx J (2007) Transcriptional coregulators in the control of energy homeostasis. *Trends Cell Biol* 17(6):292–301. <https://doi.org/10.1016/j.tcb.2007.04.001>
32. Hardie DG (2008) AMPK: a key regulator of energy balance in the single cell and the whole organism. *Int J Obes (Lond)* 32 Suppl 4:S7–12. <https://doi.org/10.1038/ijo.2008.116>
33. Fernyhough P (2015) Mitochondrial dysfunction in diabetic neuropathy: a series of unfortunate metabolic events. *Curr Diab Rep* 15(11):89. <https://doi.org/10.1007/s11892-015-0671-9>
34. Choi J, Chandrasekaran K, Inoue T, Muragundla A, Russell JW (2014) PGC-1 $\alpha$  regulation of mitochondrial degeneration in experimental diabetic neuropathy. *Neurobiol Dis* 64:118–130. <https://doi.org/10.1016/j.nbd.2014.01.001>
35. Chowdhury SK, Dobrowsky RT, Fernyhough P (2011) Nutrient excess and altered mitochondrial proteome and function contribute to neurodegeneration in diabetes. *Mitochondrion* 11(6):845–854. <https://doi.org/10.1016/j.mito.2011.06.007>
36. Aghanoori MR, Smith DR, Shariati-Ievari S, Ajisebutu A, Nguyen A, Desmond F, Jesus CHA, Zhou X et al (2019) Insulin-like growth factor-1 activates AMPK to augment mitochondrial function and correct neuronal metabolism in sensory neurons in type 1 diabetes. *Mol Metab* 20:149–165. <https://doi.org/10.1016/j.molmet.2018.11.008>
37. Chowdhury SK, Smith DR, Fernyhough P (2013) The role of aberrant mitochondrial bioenergetics in diabetic neuropathy. *Neurobiol Dis* 51:56–65. <https://doi.org/10.1016/j.nbd.2012.03.016>
38. Sabbir MG, Calcutt NA, Fernyhough P (2018) Muscarinic acetylcholine type 1 receptor activity constrains neurite outgrowth by inhibiting microtubule polymerization and mitochondrial trafficking in adult sensory neurons. *Front Neurosci* 12:402. <https://doi.org/10.3389/fnins.2018.00402>

39. Brown DA (1988) M Currents. In: Narahashi T (ed) *Ion Channels*, vol 1. Springer US, Boston, pp 55–94. [https://doi.org/10.1007/978-1-4615-7302-9\\_2](https://doi.org/10.1007/978-1-4615-7302-9_2)
40. Marrion NV (1997) Control of M-current. *Annu Rev Physiol* 59:483–504. <https://doi.org/10.1146/annurev.physiol.59.1.483>
41. Passmore GM, Selyanko AA, Mistry M, Al-Qatari M, Marsh SJ, Matthews EA, Dickenson AH, Brown TA et al (2003) KCNQ/M currents in sensory neurons: significance for pain therapy. *J Neurosci* 23(18):7227–7236. <https://doi.org/10.1523/jneurosci.23-18-07227.2003>
42. Brown DA, Adams PR (1980) Muscarinic suppression of a novel voltage-sensitive K<sup>+</sup> current in a vertebrate neurone. *Nature* 283(5748):673–676. <https://doi.org/10.1038/283673a0>
43. Brown DA, Passmore GM (2009) Neural KCNQ (Kv7) channels. *Br J Pharmacol* 156(8):1185–1195. <https://doi.org/10.1111/j.1476-5381.2009.00111.x>
44. Adams PR, Brown DA, Constanti A (1982) Pharmacological inhibition of the M-current. *J Physiol* 332:223–262. <https://doi.org/10.1113/jphysiol.1982.sp014411>
45. Marrion NV, Smart TG, Marsh SJ, Brown DA (1989) Muscarinic suppression of the M-current in the rat sympathetic ganglion is mediated by receptors of the M1-subtype. *Br J Pharmacol* 98(2):557–573. <https://doi.org/10.1111/j.1476-5381.1989.tb12630.x>
46. Miyakawa T, Yamada M, Duttaroy A, Wess J (2001) Hyperactivity and intact hippocampus-dependent learning in mice lacking the M1 muscarinic acetylcholine receptor. *J Neurosci* 21(14):5239–5250. <https://doi.org/10.1523/jneurosci.21-14-05239.2001>
47. Smiley ST, Reers M, Mottola-Hartshorn C, Lin M, Chen A, Smith TW, Steele GD Jr, Chen LB (1991) Intracellular heterogeneity in mitochondrial membrane potentials revealed by a J-aggregate-forming lipophilic cation JC-1. *Proc Natl Acad Sci U S A* 88(9):3671–3675. <https://doi.org/10.1073/pnas.88.9.3671>
48. Epps DE, Wolfe ML, Groppi V (1994) Characterization of the steady-state and dynamic fluorescence properties of the potential-sensitive dye bis-(1,3-dibutylbarbituric acid)trimethine oxonol (Dibac4(3)) in model systems and cells. *Chem Phys Lipids* 69(2):137–150. [https://doi.org/10.1016/0009-3084\(94\)90035-3](https://doi.org/10.1016/0009-3084(94)90035-3)
49. Schindelin J, Arganda-Carreras I, Frise E, Kaynig V, Longair M, Pietzsch T, Preibisch S, Rueden C et al (2012) Fiji: an open-source platform for biological-image analysis. *Nat Methods* 9(7):676–682. <https://doi.org/10.1038/nmeth.2019>
50. Lambert DG, Nahorski SR (1990) Muscarinic-receptor-mediated changes in intracellular Ca<sup>2+</sup> and inositol 1,4,5-trisphosphate mass in a human neuroblastoma cell line, SH-SY5Y. *Biochem J* 265(2):555–562. <https://doi.org/10.1042/bj2650555>
51. Murphy NP, Vaughan PF, Ball SG, McCormack JG (1991) The cholinergic regulation of intracellular calcium in the human neuroblastoma, SH-SY5Y. *J Neurochem* 57(6):2116–2123. <https://doi.org/10.1111/j.1471-4159.1991.tb06430.x>
52. Gómez-Ramos A, Díaz-Hernández M, Rubio A, Miras-Portugal MT, Avila J (2008) Extracellular tau promotes intracellular calcium increase through M1 and M3 muscarinic receptors in neuronal cells. *Mol Cell Neurosci* 37(4):673–681. <https://doi.org/10.1016/j.mcn.2007.12.010>
53. Herzig S, Shaw RJ (2018) AMPK: guardian of metabolism and mitochondrial homeostasis. *Nat Rev Mol Cell Biol* 19(2):121–135. <https://doi.org/10.1038/nrm.2017.95>
54. Jornayvaz FR, Shulman GI (2010) Regulation of mitochondrial biogenesis. *Essays Biochem* 47:69–84. <https://doi.org/10.1042/bse0470069>
55. Fulda S, Gorman AM, Hori O, Samali A (2010) Cellular stress responses: cell survival and cell death. *Int J Cell Biol* 2010:214074. <https://doi.org/10.1155/2010/214074>
56. Zorova LD, Popkov VA, Plotnikov EY, Silachev DN, Pevzner IB, Jankauskas SS, Babenko VA, Zorov SD et al (2018) Mitochondrial membrane potential. *Anal Biochem* 552:50–59. <https://doi.org/10.1016/j.ab.2017.07.009>
57. Green DR, Reed JC (1998) Mitochondria and apoptosis. *Science* 281(5381):1309–1312. <https://doi.org/10.1126/science.281.5381.1309>
58. Yin K, Baillie GJ, Vetter I (2016) Neuronal cell lines as model dorsal root ganglion neurons: a transcriptomic comparison. *Mol Pain* 12. <https://doi.org/10.1177/1744806916646111>
59. Chen W, Mi R, Haughey N, Oz M, Hoke A (2007) Immortalization and characterization of a nociceptive dorsal root ganglion sensory neuronal line. *J Peripher Nerv Syst* 12(2):121–130. <https://doi.org/10.1111/j.1529-8027.2007.00131.x>
60. Butcher AJ, Bradley SJ, Prihandoko R, Brooke SM, Mogg A, Bourgognon JM, Macedo-Hatch T, Edwards JM et al (2016) An antibody biosensor establishes the activation of the M1 muscarinic acetylcholine receptor during learning and memory. *J Biol Chem* 291(17):8862–8875. <https://doi.org/10.1074/jbc.M115.681726>
61. Cashman CR, Höke A (2015) Mechanisms of distal axonal degeneration in peripheral neuropathies. *Neurosci Lett* 596:33–50. <https://doi.org/10.1016/j.neulet.2015.01.048>
62. Lashin OM, Szweda PA, Szweda LI, Romani AM (2006) Decreased complex II respiration and HNE-modified SDH subunit in diabetic heart. *Free Radic Biol Med* 40(5):886–896. <https://doi.org/10.1016/j.freeradbiomed.2005.10.040>
63. Mogensen M, Sahlin K, Fernström M, Glinborg D, Vind BF, Beck-Nielsen H, Højlund K (2007) Mitochondrial respiration is decreased in skeletal muscle of patients with type 2 diabetes. *Diabetes* 56(6):1592–1599. <https://doi.org/10.2337/db06-0981>
64. Fink B, Coppel L, Davidson E, Shevalye H, Obrosova A, Chheda PR, Kerns R, Sivitz W et al (2020) Effect of mitoquinone (Mito-Q) on neuropathic endpoints in an obese and type 2 diabetic rat model. *Free Radic Res* 54(5):311–318. <https://doi.org/10.1080/10715762.2020.1754409>
65. Vaarmann A, Mandel M, Zeb A, Wareski P, Liiv J, Kuum M, Antsov E, Liiv M et al (2016) Mitochondrial biogenesis is required for axonal growth. *Development* 143(11):1981–1992. <https://doi.org/10.1242/dev.128926>
66. Wu Z, Puigserver P, Andersson U, Zhang C, Adelmant G, Mootha V, Troy A, Cinti S et al (1999) Mechanisms controlling mitochondrial biogenesis and respiration through the thermogenic coactivator PGC-1. *Cell* 98(1):115–124. [https://doi.org/10.1016/s0092-8674\(00\)80611-x](https://doi.org/10.1016/s0092-8674(00)80611-x)
67. Dasgupta B, Milbrandt J (2007) Resveratrol stimulates AMP kinase activity in neurons. *Proc Natl Acad Sci U S A* 104(17):7217–7222. <https://doi.org/10.1073/pnas.0610068104>
68. Ortiz Mdel C, Lores-Arnaiz S, Albertoni Borghese MF, Balonga S, Lavagna A, Filipuzzi AL, Cicerchia D, Majowicz M et al (2013) Mitochondrial dysfunction in brain cortex mitochondria of STZ-diabetic rats: effect of L-Arginine. *Neurochem Res* 38(12):2570–2580. <https://doi.org/10.1007/s11064-013-1172-3>
69. Scaduto RC Jr, Grotzjahn LW (1999) Measurement of mitochondrial membrane potential using fluorescent rhodamine derivatives. *Biophys J* 76(1 Pt 1):469–477. [https://doi.org/10.1016/s0006-3495\(99\)77214-0](https://doi.org/10.1016/s0006-3495(99)77214-0)
70. Delmas P, Brown DA (2005) Pathways modulating neural KCNQ/M (Kv7) potassium channels. *Nat Rev Neurosci* 6(11):850–862. <https://doi.org/10.1038/nrn1785>
71. Constanti A, Brown DA (1981) M-Currents in voltage-clamped mammalian sympathetic neurones. *Neurosci Lett* 24(3):289–294. [https://doi.org/10.1016/0304-3940\(81\)90173-7](https://doi.org/10.1016/0304-3940(81)90173-7)
72. Bernheim L, Mathie A, Hille B (1992) Characterization of muscarinic receptor subtypes inhibiting Ca<sup>2+</sup> current and M current in rat sympathetic neurons. *Proc Natl Acad Sci U S A* 89(20):9544–9548. <https://doi.org/10.1073/pnas.89.20.9544>



73. Jones S, Brown DA, Milligan G, Willer E, Buckley NJ, Caulfield MP (1995) Bradykinin excites rat sympathetic neurons by inhibition of M current through a mechanism involving B2 receptors and G alpha q/11. *Neuron* 14(2):399–405. [https://doi.org/10.1016/0896-6273\(95\)90295-3](https://doi.org/10.1016/0896-6273(95)90295-3)
74. Wang HS, McKinnon D (1995) Potassium currents in rat prevertebral and paravertebral sympathetic neurones: control of firing properties. *J Physiol* 485(Pt 2):319–335. <https://doi.org/10.1113/jphysiol.1995.sp020732>
75. Shapiro MS, Roche JP, Kaftan EJ, Cruzblanca H, Mackie K, Hille B (2000) Reconstitution of muscarinic modulation of the KCNQ2/KCNQ3 K(+) channels that underlie the neuronal M current. *J Neurosci* 20(5):1710–1721. <https://doi.org/10.1523/jneurosci.20-05-01710.2000>
76. Li Y, Gamper N, Hilgemann DW, Shapiro MS (2005) Regulation of Kv7 (KCNQ) K+ channel open probability by phosphatidylinositol 4,5-bisphosphate. *J Neurosci* 25(43):9825–9835. <https://doi.org/10.1523/jneurosci.2597-05.2005>
77. Zhang H, Craciun LC, Mirshahi T, Rohács T, Lopes CM, Jin T, Logothetis DE (2003) PIP(2) activates KCNQ channels, and its hydrolysis underlies receptor-mediated inhibition of M currents. *Neuron* 37(6):963–975. [https://doi.org/10.1016/s0896-6273\(03\)00125-9](https://doi.org/10.1016/s0896-6273(03)00125-9)
78. Malhotra RK, Bhave SV, Wakade TD, Bhave AS, Wakade AR (1990) Effects of neurotransmitters and peptides on phospholipid hydrolysis in sympathetic and sensory neurons. *FASEB J* 4(8):2492–2498. <https://doi.org/10.1096/fasebj.4.8.1970791>
79. Hoshi N, Zhang JS, Omaki M, Takeuchi T, Yokoyama S, Wanaverbecq N, Langeberg LK, Yoneda Y et al (2003) AKAP150 signaling complex promotes suppression of the M-current by muscarinic agonists. *Nat Neurosci* 6(6):564–571. <https://doi.org/10.1038/nm1062>
80. Borgini M, Mondal P, Liu R, Wipf P (2021) Chemical modulation of Kv7 potassium channels. *RSC Med Chem* 12(4):483–537. <https://doi.org/10.1039/d0md00328j>
81. Greene DL, Hoshi N (2017) Modulation of Kv7 channels and excitability in the brain. *Cell Mol Life Sci* 74(3):495–508. <https://doi.org/10.1007/s00018-016-2359-y>
82. Suh BC, Inoue T, Meyer T, Hille B (2006) Rapid chemically induced changes of PtdIns(4,5)P2 gate KCNQ ion channels. *Science* 314(5804):1454–1457. <https://doi.org/10.1126/science.1131163>
83. Winks JS, Hughes S, Filippov AK, Tatulian L, Abogadie FC, Brown DA, Marsh SJ (2005) Relationship between membrane phosphatidylinositol-4,5-bisphosphate and receptor-mediated inhibition of native neuronal M channels. *J Neurosci* 25(13):3400–3413. <https://doi.org/10.1523/jneurosci.3231-04.2005>
84. Peiris M, Hockley JR, Reed DE, Smith ESJ, Bulmer DC, Blackshaw LA (2017) Peripheral K(V)7 channels regulate visceral sensory function in mouse and human colon. *Mol Pain* 13:1744806917709371. <https://doi.org/10.1177/1744806917709371>
85. Passmore GM, Reilly JM, Thakur M, Keasberry VN, Marsh SJ, Dickenson AH, Brown DA (2012) Functional significance of M-type potassium channels in nociceptive cutaneous sensory endings. *Front Mol Neurosci* 5:63. <https://doi.org/10.3389/fnmol.2012.00063>
86. Pan Z, Kao T, Horvath Z, Lemos J, Sul JY, Cranstoun SD, Bennett V, Scherer SS et al (2006) A common ankyrin-G-based mechanism retains KCNQ and NaV channels at electrically active domains of the axon. *J Neurosci* 26(10):2599–2613. <https://doi.org/10.1523/jneurosci.4314-05.2006>
87. Yue C, Yaari Y (2004) KCNQ/M channels control spike afterdepolarization and burst generation in hippocampal neurons. *J Neurosci* 24(19):4614–4624. <https://doi.org/10.1523/jneurosci.0765-04.2004>
88. Rivera-Arconada I, Lopez-Garcia JA (2006) Retigabine-induced population primary afferent hyperpolarisation in vitro. *Neuropharmacology* 51(4):756–763. <https://doi.org/10.1016/j.neuropharm.2006.05.015>
89. Lang PM, Fleckenstein J, Passmore GM, Brown DA, Grafe P (2008) Retigabine reduces the excitability of unmyelinated peripheral human axons. *Neuropharmacology* 54(8):1271–1278. <https://doi.org/10.1016/j.neuropharm.2008.04.006>
90. Roza C, Lopez-Garcia JA (2008) Retigabine, the specific KCNQ channel opener, blocks ectopic discharges in axotomized sensory fibres. *Pain* 138(3):537–545. <https://doi.org/10.1016/j.pain.2008.01.031>
91. Wainger BJ, Kiskinis E, Mellin C, Wiskow O, Han SS, Sandoe J, Perez NP, Williams LA et al (2014) Intrinsic membrane hyperexcitability of amyotrophic lateral sclerosis patient-derived motor neurons. *Cell Rep* 7(1):1–11. <https://doi.org/10.1016/j.celrep.2014.03.019>
92. Tzour A, Leibovich H, Barkai O, Biala Y, Lev S, Yaari Y, Binshtok AM (2017) K(V) 7/M channels as targets for lipopolysaccharide-induced inflammatory neuronal hyperexcitability. *J Physiol* 595(3):713–738. <https://doi.org/10.1113/jp272547>
93. Zheng Q, Fang D, Liu M, Cai J, Wan Y, Han JS, Xing GG (2013) Suppression of KCNQ/M (Kv7) potassium channels in dorsal root ganglion neurons contributes to the development of bone cancer pain in a rat model. *Pain* 154(3):434–448. <https://doi.org/10.1016/j.pain.2012.12.005>
94. Zheng Y, Xu H, Zhan L, Zhou X, Chen X, Gao Z (2015) Activation of peripheral KCNQ channels relieves gout pain. *Pain* 156(6):1025–1035. <https://doi.org/10.1097/j.pain.0000000000000122>
95. Vigil FA, Carver CM, Shapiro MS (2020) Pharmacological manipulation of K (v) 7 channels as a new therapeutic tool for multiple brain disorders. *Front Physiol* 11:688. <https://doi.org/10.3389/fphys.2020.00688>
96. Barkai O, Goldstein RH, Caspi Y, Katz B, Lev S, Binshtok AM (2017) The role of Kv7/M potassium channels in controlling ectopic firing in nociceptors. *Front Mol Neurosci* 10:181. <https://doi.org/10.3389/fnmol.2017.00181>
97. King CH, Lancaster E, Salomon D, Peles E, Scherer SS (2014) Kv7.2 regulates the function of peripheral sensory neurons. *J Comp Neurol* 522(14):3262–3280. <https://doi.org/10.1002/cne.23595>
98. Duncan C, Mueller S, Simon E, Renger JJ, Uebele VN, Hogan QH, Wu HE (2013) Painful nerve injury decreases sarco-endoplasmic reticulum Ca<sup>2+</sup>-ATPase activity in axotomized sensory neurons. *Neuroscience* 231:247–257. <https://doi.org/10.1016/j.neuroscience.2012.11.055>
99. Devor M, McMahon S, Koltzenburg M (2006) Wall and Melzack's textbook of pain. Elsevier, Beijing
100. Devor M (2009) Ectopic discharge in Abeta afferents as a source of neuropathic pain. *Exp Brain Res* 196(1):115–128. <https://doi.org/10.1007/s00221-009-1724-6>
101. Liu CN, Michaelis M, Amir R, Devor M (2000) Spinal nerve injury enhances subthreshold membrane potential oscillations in DRG neurons: relation to neuropathic pain. *J Neurophysiol* 84(1):205–215. <https://doi.org/10.1152/jn.2000.84.1.205>
102. Bernstein BW, Bamberg JR (2003) Actin-ATP hydrolysis is a major energy drain for neurons. *J Neurosci* 23(1):1–6. <https://doi.org/10.1523/jneurosci.23-01-00002.2003>
103. Paventi G, Soldovieri MV, Servetini I, Barrese V, Miceli F, Sisalli MJ, Ambrosino P, Mosca I et al (2022) Kv74 channels regulate potassium permeability in neuronal mitochondria. *Biochem Pharmacol* 197:114931. <https://doi.org/10.1016/j.bcp.2022.114931>

**Publisher's Note** Springer Nature remains neutral with regard to jurisdictional claims in published maps and institutional affiliations.